

Early stage of Ge growth on Si(001) vicinal surfaces with an 8° miscut along [110]

P. D. Szkutnik,* A. Sgarlata, and A. Balzarotti

Dipartimento di Fisica, Università di Roma Tor Vergata, Via della Ricerca Scientifica 1, 00133 Roma, Italy

N. Motta

School of Engineering Systems, Queensland University of Technology, GPO Box 2434, Brisbane Qld 4001, Australia

A. Ronda† and I. Berbezier†

L2MP, CNRS UMR 6137, Faculté des Sciences St Jérôme, Avenue Escadrille Normandie Niemen-Case 142, 13397 Marseille Cedex 20, France

(Received 23 January 2006; revised manuscript received 20 July 2006; published 9 January 2007)

The atomistic pathway towards the growth of semiconductors heterostructures on vicinal surfaces is investigated in a special experiment. A step-by-step study of the early stages of Ge deposition at $T=873$ K on a 8° off Si(001) surface miscut along [110] is performed by scanning tunneling microscopy (STM). The microscopic processes occurring during growth are identified. Highly resolved STM images show how double height steps, which characterize the clean substrate, evolve by a step flow process generated by addimer chains located at specific positions. This process leads to the formation of metastable single domains until the development of {105} faceted ripples extending along the whole surface in the miscut direction.

DOI: 10.1103/PhysRevB.75.033305

PACS number(s): 68.55.Ac, 68.37.Ef, 68.65.-k

Heteroepitaxy on vicinal semiconductor surfaces has been extensively studied as a means of texturing surfaces^{1–4} for device applications through the exploitation of growth instabilities.^{5,6} In the case of Ge growth on low miscut Si(001) surfaces, different mechanisms have been proposed as responsible for such instabilities: for example, strain-induced step bunching,⁷ step-edge barriers,⁸ and kinetic effects⁹ such as diffusion anisotropy.¹⁰ At high miscut a complex situation is found wherein the interplay between incorporation of adatoms, surface reconstruction, miscut azimuth, and growth conditions result in a rippled morphology.^{6,10–15} At the mesoscopic level, the ripples appear elongated either perpendicular to or along the miscut direction, depending on whether the miscut angle is smaller than or larger than $\sim 5^\circ$.^{4,15} In principle, strain release via step bunching should predominate due to the high density of steps. For instance, in corrugated Si layers with 4° miscut angle, strain relaxation is achieved by the coalescence of step bunches to form ridge structures perpendicular to the miscut direction with two low energy {105} facets inclined at 8° with respect to the (001) plane.¹¹

The purpose of this paper is to study the ripple formation on 8° miscut Si(001) surface with atomic resolution at the very early stages of growth which seem to provide the essential elements for the initial roughening.¹⁶ The deposition of Ge in the absence of a silicon buffer layer suppresses Si kinetic step bunching.⁹ We have chosen an 8° off Si(001) surface for several reasons. First, the surface morphology upon overgrowth with a strained SiGe layer presents a single symmetry because the surface consists of double-height steps (D_B)^{17,18} instead of the alternate smooth and rough single S_A and S_B steps.¹⁹ Second, the 8° off miscut is of special interest because the [551] intersection line between the (105) and (0 $\bar{1}$ 5) facets of the Ge hut clusters on flat Si(001) surfaces^{20–22} forms approximately an 8° angle with the (001) plane. This makes the surface unstable as regards {105} face-

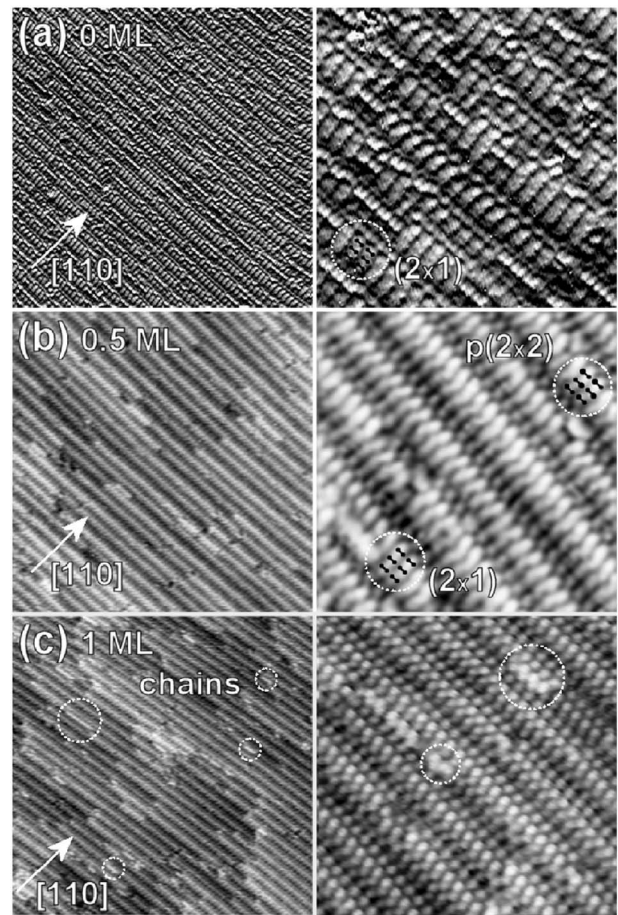


FIG. 1. (a) STM filled-state images ($V_{\text{bias}}=-1.8$ V) of the clean 8° off Si(001) surface. (b) After 0.5 ML and (c) after 1 ML of Ge deposited at 873 K. Zigzag chains and dimer rows are highlighted. Scan areas are 50×50 nm² (left column) and 15×15 nm² (right column).

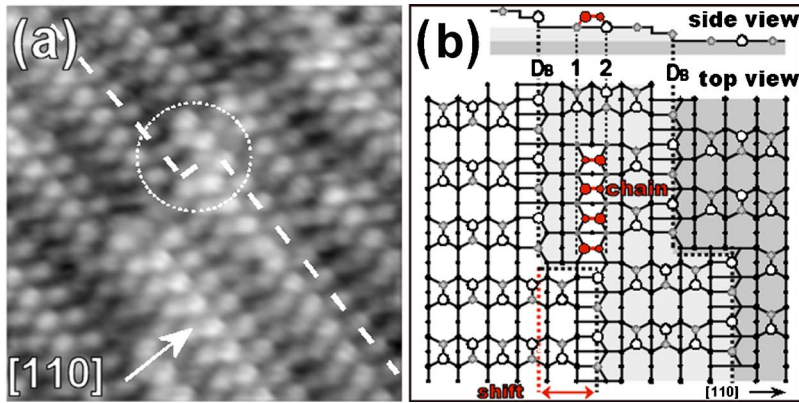


FIG. 2. (Color online) (a) STM image $10 \times 10 \text{ nm}^2$ of the vicinal Si(001) surface covered by 1 ML of Ge. The step edge shift by a distance of two lattice parameters and the zigzag chain are highlighted (dashed ring). (b) Schematic representation (side view and top view) of the step edge shift and of dimers forming the zigzag chain. Grey shades indicate different atomic planes.

ting; consequently, long ripples are formed by the faceted ridges in the miscut direction.^{13–15}

Experiments were carried out in the ultrahigh vacuum (2×10^{-11} mbar) chamber of a variable temperature scanning tunneling microscope (STM). *P*-type *B*-doped Si(001) wafers with a 8° miscut angle towards the [110] direction were cleaned *in situ* by thermal annealing at 1473 K. Ge was deposited by physical vapor deposition at a growth temperature of 873 K with a constant flux of 1.25×10^{-2} ML/s to suppress kinetic step bunching.¹⁰ A series of STM snapshots at room temperature were recorded after each deposition in order to image the morphology of the surface at every stage. To enhance surface reconstruction a suitable background level was subtracted by a flatten filtering procedure. By means of STM we track the morphological evolution of the Si surface up to 6 monolayers (MLs) of Ge. The results show that short zigzag chains of Ge adatoms trigger the flow of double steps, this leading to the formation of metastable domains all of which are aligned along the miscut direction [110]. Afterwards the surface suddenly roughens due to the appearance of {105} facets on domain sidewalls perpendicular to the steps. The faceted domains (ripples) are elongated parallel to the miscut direction and contain a large number of D_B steps with the step edge perpendicular to the miscut direction. The ripple orientation period and height are consistent with patterns observed on high miscut surfaces with thicker Ge layers,^{1,6,15} but do not need preexisting step bunches for their description.

Typical filled-states STM images of the clean vicinal surface are presented in Fig. 1(a). The measured average local slope of the surface toward [110] is 7.7° . We find terraces $2.0 \pm 0.2 \text{ nm}$ wide with dimer bonds parallel to the step edge and D_B steps. The rows on each terrace, consisting of a series of three dimers, are separated by $0.78 \pm 0.01 \text{ nm}$.

After deposition of 0.5 ML of Ge [Fig. 1(b)], the train of D_B steps becomes more regular implying a strong reduction in the defect density. Instead of the usual (2×1) reconstruction of terraces, the $p(2 \times 2)$ reconstruction is observed. At 1 ML coverage, the $p(2 \times 2)$ reconstruction covers the whole surface and single atoms protrude at the step edge [Fig. 1(c)]. The dimer row separation is $0.68 \pm 0.01 \text{ nm}$, smaller than that of the clean surface, so matching the measured periodicity of the upper rebonded atom at the D_B step edge. Moreover, short zigzag chains appear on the terraces [see schematics in Fig. 2]. At 2 ML coverage, domains composed of D_B steps

shifted by a distance of two lattice parameters [Fig. 3(a), right] advance over the surface toward the miscut direction showing a step flow process. At 3 ML coverage the domains appear elongated toward the miscut direction and have irregular borders in the other directions [Fig. 3(b)]. They consist of D_B steps, all equally shifted in the [110] direction. At 4 ML coverage [Fig. 3(c)] an abrupt morphological transition takes place: A few domains present {105} facets oriented perpendicularly to the edge of the D_B steps. These facets extend

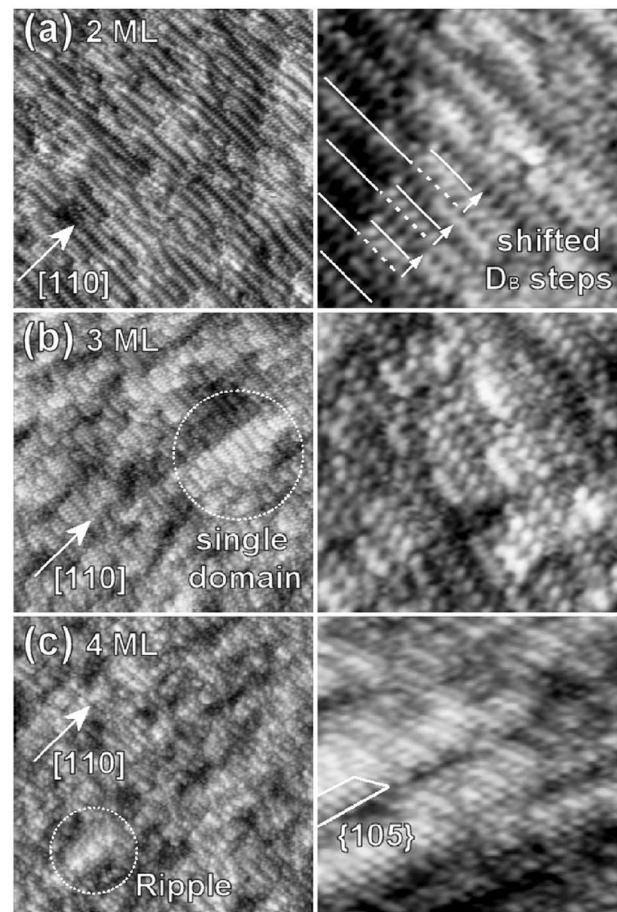


FIG. 3. STM images ($V_{\text{bias}} = -1.8 \text{ V}$) of the vicinal 8° off Si(001) surface after different Ge deposition at 873 K: (a) 2 ML; (b) 3 ML; (c) 4 ML. The propagation direction of the step edge; a single domain, a ripple, and a {105} facet are evidenced. Scan areas are $50 \times 50 \text{ nm}^2$ (left column) and $15 \times 15 \text{ nm}^2$ (right column).

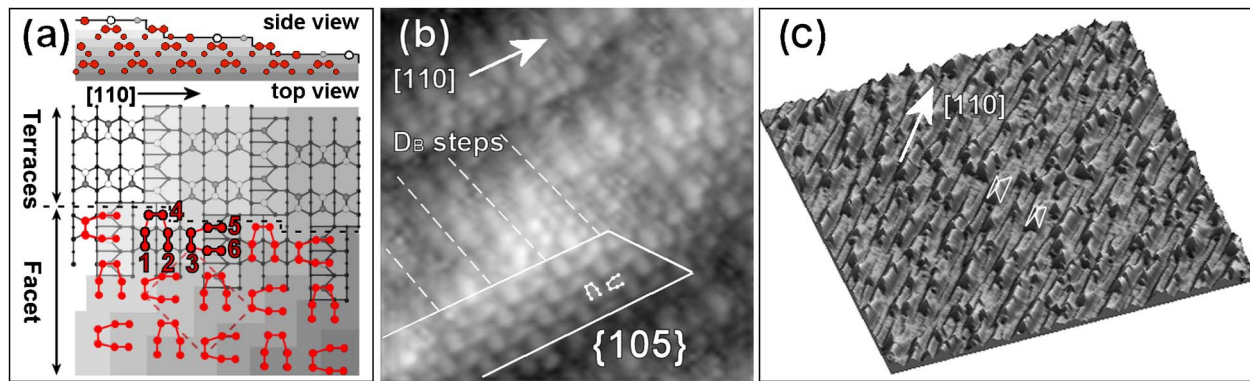


FIG. 4. (Color online) (a) Schematic view of the top of the uncompleted ripple, composed of terraces and a $\{105\}$ reconstructed facet. The different grey levels indicate different atomic planes. The rectangular RS surface unit cell is shown (red dashed line). (b) STM image $15 \times 15 \text{ nm}^2$ ($V_{\text{bias}} = -1.9 \text{ V}$) for a coverage of 6 MLs showing a partial $\{105\}$ facet and D_B steps with two RS structures evidenced. (c) STM image $500 \times 500 \text{ nm}^2$: three dimensional view of the rippled surface with two ripples evidenced.

along the miscut direction, forming elongated ripples [Fig. 3(c)].

The morphology of the clean surface (step height and terrace width), shown in Fig. 1(a), agrees with that predicted for a Si(001) substrate with a miscut angle of 8° on which we have deposited Ge without any Si buffer layer.

At submonolayer Ge deposition the appearance of the $p(2 \times 2)$ reconstruction on the terraces, shown in Fig. 1(b), can be explained as resulting from an intermixing process²³ and implies the formation of Ge-Ge or Ge-Si dimers where Ge is the uppermost atom.²⁴ Theoretical calculations by Lee *et al.*²⁵ show that at low Ge coverage the $p(2 \times 2)$ reconstruction is the most energetically favorable. Furthermore, as reported by Kim *et al.*,²⁶ rebonding at D_B step edges, which generates a 4% elongation of Si bonds, provides vacancy sites well suited for Ge incorporation. All these findings suggest that Ge is incorporated at the step-edge sites²⁷ by replacing a Si atom in order to reduce the bond distortion energy of the (2×1) reconstruction. Such a process explains the uniformity of the terraces and the straightness of the step edge shown in Fig. 1(b).

The appearance of one-ML-high zigzag chains, at 1 ML coverage, indicates that growth proceeds by rearranging Ge atoms over the surface [Fig. 1(c)]. Chains are composed of addimers perpendicular to the dimers of the terraces [Fig. 2(b)]. Their variable length suggests that they originate from an aggregation process of single addimers, as is supported by previous works^{25,28,29} on different configurations of Ge and Si addimers on the Si(001) surface. Nevertheless, in our case, chains have a preferential attachment site, as schematically illustrated in Fig. 2(b). Taking the edge of the D_B step as a reference point, the zigzag chain is located two lattice parameters away from the step edge. The zigzag chain consists of dimers located in two alternate positions between dimers 1 and 2 of the terrace: One dimer is situated within a row of the $p(2 \times 2)$ reconstruction and corresponds to the most stable configuration^{28,29} while the other one lies between two adjacent rows. Taken together, they form a chain which reduces the tensile strain energy of dimer bonds located along the base of the D_B step edges, particularly for small terrace widths.⁷ It must be noted that the position of

the shifted step edge coincides with that of the zigzag chain which behaves as an epitaxial segment.²⁹ So zigzag chains allow the enlargement of the upper terrace and promote the shift of the D_B step edge, starting the step flow process. By increasing the coverage, the flow of regular trains of D_B steps produces the disconnected domains seen in Fig. 3(b) over which new zigzag chains form until, at 4 ML coverage, the domains develop reconstructed $\{105\}$ facets.

To model the formation of ripples which consist of terraces and reconstructed facets, as shown in Fig. 4(b), we consider terraces with D_B steps shifted by a distance of two lattice parameters and a portion of the rebonded-step (RS)³⁰ reconstructed facet illustrated schematically in Fig. 4(a). On this facet the dimers labeled 1-2-3 of the RS structure correspond to those of the $p(2 \times 2)$ surface reconstruction. The addimer labeled 4 belongs to the zigzag chain while the last two dimers (labeled 5-6), being perpendicular to the $p(2 \times 2)$ dimers, presumably result from the rearrangement of the D_B step into two monoatomic S_A and S_B steps.^{17,18} Since the configuration with the type 4 addimer isolated is unfavored,²⁹ D_B steps must accumulate. By increasing the coverage, the addition of type 4 addimers widens the $\{105\}$ facet and increases the height of the ripple. Meanwhile, the train of shifted D_B steps propagate itself inducing the elongation of the ripple in the miscut direction. The lateral $\{105\}$ facets perpendicular to the step extend in height until they meet at the top. On an expanded scale, a surface with reconstructed ripples oriented along the $[110]$ direction is finally obtained at 6 ML coverage, as displayed in Fig. 4(c). The average width of the ripples is about 40 nm.

In conclusion, the microscopic roughening process of a vicinal 8° off Si(001) surface is followed, step-by-step, starting from submonolayer coverage of Ge until the formation of Three-dimensional ripples bordered by two $\{105\}$ reconstructed facets perpendicular to the step edges. This evolution is driven by zigzag chains located at specific sites on the surface. In the absence of step bunching, we find that the ripples elongate by means of a step-flow process of double steps which occurs in the miscut direction. Proceeding with Ge deposition, two $\{105\}$ facets appear at the base of each

ripple, most likely to reduce the strain energy of the Si-Ge interface. In order to further relax the strain associated with the increased surface area, the facets reconstruct, forming the characteristic structures evidenced in Fig. 4(b). We would like to emphasize that the microscopic corrugation occurs through a step flow process under a diffusion bias in the miscut direction. At larger Ge depositions, the rippled morphology evolves towards the ordered templates of SiGe

nanowires which are oriented along the miscut direction and tailored for self-organized island deposition.^{2,4}

The authors are grateful to Martin Bennett and to Megan Portavoce Smith for a critical reading of the manuscript. This work was supported by the European Community (EC) through FORUM-FIB contract (Contract No. IST-2000-29573) at the Roma Tor Vergata University.

*Corresponding author. Electronic address: pierre.szcutnik@l2mp.fr

[†]On leave from CRMCN-CNRS, Campus Luminy, case 913, F-13288 Marseille cedex 9, France.

¹C. Teichert, *Phys. Rep.* **365**, 335 (2002).

²A. Ronda and I. Berbezier, *Physica E (Amsterdam)* **6**, 370 (2004).

³J. Zhu, K. Brunner, and G. Abstreiter, *Appl. Phys. Lett.* **73**, 620 (1998).

⁴I. Berbezier, A. Ronda, A. Portavoce, and N. Motta, *Appl. Phys. Lett.* **83**, 4833 (2003).

⁵G. S. Bales and A. Zangwill, *Phys. Rev. B* **41**, 5500 (1990).

⁶I. Berbezier, B. Gallas, L. Lapena, J. Fernandez, J. Derrien, and B. Joyce, *J. Vac. Sci. Technol. B* **16**, 1582 (1998).

⁷J. Tersoff, Y. H. Phang, Zhenyu Zhang, and M. G. Lagally, *Phys. Rev. Lett.* **75**, 2730 (1995).

⁸A. Pimpinelli and A. Videcoq, *Surf. Sci.* **445**, L23 (2000).

⁹C. Schelling, M. Mühlberger, G. Springholz, and F. Schäffler, *Phys. Rev. B* **64**, 041301(R) (2001).

¹⁰J. Myslivecek, C. Schelling, F. Schäffler, G. Springholz, P. Smilauer, J. Krug, and B. Voigtländer, *Surf. Sci.* **520**, 193 (2002).

¹¹H. Lichtenberger, M. Mühlberger, and F. Schäffler, *Appl. Phys. Lett.* **86**, 131919 (2005).

¹²C. Teichert, J. C. Bean, and M. G. Lagally, *Appl. Phys. A: Mater. Sci. Process.* **67**, 675 (1998).

¹³I. Berbezier, A. Ronda, F. Volpi, and A. Portavoce, *Surf. Sci.* **531**, 231 (2003).

¹⁴L. W. Guo, N. Lin, Q. Huang, J. M. Zhou, and N. Cue, *Appl. Surf. Sci.* **126**, 213 (1998).

¹⁵F. Watanabe, D. G. Cahill, S. Hong, and J. E. Greene, *Appl. Phys. Lett.* **85**, 1238 (2004).

¹⁶P. Sutter, I. Schick, W. Ernst, and E. Sutter, *Phys. Rev. Lett.* **91**, 176102 (2003).

¹⁷B. S. Swartzentruber, N. Kitamura, M. G. Lagally, and M. B. Webb, *Phys. Rev. B* **47**, 13432 (1993).

¹⁸O. L. Alerhand, A. N. Berker, J. D. Joannopoulos, David Vanderbilt, R. J. Hamers, and J. E. Demuth, *Phys. Rev. Lett.* **64**, 2406 (1990), and references therein.

¹⁹D. J. Chadi, *Phys. Rev. Lett.* **59**, 1691 (1987).

²⁰Y-W. Mo, D. E. Savage, B. S. Swartzentruber, and M. G. Lagally, *Phys. Rev. Lett.* **65**, 1020 (1990).

²¹P. Sutter, P. Zahl, and E. Sutter, *Appl. Phys. Lett.* **82**, 3454 (2003).

²²P. D. Szcutnik, A. Sgarlata, S. Nufri, N. Motta, and A. Balzarotti, *Phys. Rev. B* **69**, 201309(R) (2004).

²³X. R. Qin, B. S. Swartzentruber, and M. G. Lagally, *Phys. Rev. Lett.* **84**, 4645 (2000).

²⁴X. Chen, D. K. Saldin, E. L. Bullock, L. Patthey, L. S. O. Johansson, J. Tani, T. Abukawa, and S. Kono, *Phys. Rev. B* **55**, R7319 (1997).

²⁵S. M. Lee, E. Kim, Y. H. Lee, and N-G. Kim, *J. Korean Phys. Soc.* **33**, 684 (1998).

²⁶E. Kim, C. W. Oh, and Y. H. Lee, *Phys. Rev. Lett.* **79**, 4621 (1997).

²⁷The strong reactivity of step edge was demonstrated by theoretical and experimental works on hydrogen adsorption [M. Dürr, Z. Hu, A. Biedermann, U. Höfer and T. F. Heinz, *Phys. Rev. B* **63**, 121315(R) (2001); P. Kratzer, E. Pehlke, M. Scheffler, M. B. Raschke, and U. Höfer, *Phys. Rev. Lett.* **81**, 5596 (1998)].

²⁸Z-Y. Lu, C-Z. Wang, and K-M. Ho, *Phys. Rev. B* **62**, 8104 (2000), and references therein.

²⁹J. van Wingerden, A. van Dam, M. J. Haye, P. M. L. O. Scholte, and F. Tuinstra, *Phys. Rev. B* **55**, 4723 (1997).

³⁰P. Raiteri, D. B. Migas, Leo Miglio, A. Rastelli, and H. von Känel, *Phys. Rev. Lett.* **88**, 256103 (2002), and references therein.